Chemical Physics Letters 713 (2018) 153–159

Contents lists available at ScienceDirect

Chemical Physics Letters

journal homepage: www.elsevier.com/locate/cplett

Research paper

First principles calculations of interfacial properties and electronic structure of the AlN(0 0 0 1)/Ti(0 0 0 1) interface

Weichao Jin[a,1], Lei Li[a,1], Shanshan Zhang[a], Huisheng Yang[a], Kewei Gao[a], Xiaolu Pang[a,*], Alex A. Volinsky[b]

[a] School of Materials Science and Engineering, University of Science and Technology Beijing, Beijing 100083, China
[b] Department of Mechanical Engineering, University of South Florida, Tampa, FL 33620, USA

HIGHLIGHTS

- Two terminations and different stacking sequences were investigated.
- Six possible interface models were established.
- Termination structure played an important role on the interfacial stability.
- The electronic structure and bonding nature were investigated.
- The most stability of AlN/Ti interface module was established.
- The most stability of AlN/Ti interface show high charge transfer.

ARTICLE INFO

Keywords:
First principles
Interface
Work of separation
Electronic structure

ABSTRACT

The first principles calculations were performed to obtain the ideal work of separation (W_{sep}), electronic structure and the bonding nature of the AlN(0 0 0 1)/Ti(0 0 0 1) interface. Taking into account two terminations of AlN(0 0 0 1) and different stacking sequences, six possible interface models were investigated. The W_{sep} and interfacial distance indicated (d_0) that terminated structure and stacking sequence both played a significant role on the interfacial stability. Moreover, the N-terminated interfaces with TL stacking sequence presented larger W_{sep} and shorter d_0 than other structures. Furthermore, the electronic structure suggested that the strongest covalent interfacial bond is largely affected by the N-p and Ti-d hybridizations.

1. Introduction

With the increasing demands of high power density, frequency, efficiency and reliability of high power electronic devices, ceramics with high thermal conductivity, low coefficient of thermal expansion (CTE), and excellent heat and chemical resistance are used for high power module applications, such as LED lighting and insulated gate bipolar transistor (IGBT) packaging [1,2]. Compared with conventional plastic-based printed circuit board (PCB), direct-plated-copper (DPC) and direct-bonded copper (DBC) are promising techniques for electronic packaging [3]. The DPC aluminum nitride (AlN) substrate with high thermal conductivity (k = 170 W/m K) provides a good alternative to conventional aluminum oxide (Al_2O_3) substrate (k = 24 W/m K) for better heat dissipation [4]. As a DPC substrate, it is crucial for AlN ceramics to have good bonding with transition metals, but the two are hard to combine. Consequently, theoretical research of AlN-metal interface is necessary.

In DPC ceramic substrate systems, sputtered Ti is often used as the interfacial material between Cu and ceramic substrate [5]. Ti has lower strength and hardness than AlN ceramics. Therefore, metal-ceramic multilayers, such as Ti and AlN, have advantages of both types of materials. The interfacial structure and electronic properties of the AlN/Ti interface play a crucial role in determining the interfacial adhesion properties. Some researchers have studied thermal cyclic loading and delamination failures of AlN substrate experimentally [6]. Unfortunately, the factors affecting the interfacial properties are still poorly understood. To optimize preparation techniques and understand influencing factors, the AlN/Ti interface should be better studied.

* Corresponding author.
E-mail address: pangxl@mater.ustb.edu.cn (X. Pang).
[1] These authors contributed equally to this work and should be considered first co-authors.

https://doi.org/10.1016/j.cplett.2018.10.034
Received 25 July 2018; Accepted 11 October 2018
Available online 12 October 2018
0009-2614/

First principles calculations based on the density functional theory (DFT) are a powerful tool to calculate the interfacial properties, with many results obtained regarding atomic configuration and even electronic distribution. The recent paper dealing with ceramic-metal interface accurately estimated the interfacial stability and interfacial structure [8–10]. Numerous first principles calculations based on the DFT have been applied to metal-ceramic interfaces. Siegel et al. [7] built a small database of the work of adhesion for Al/nitrides (VN, CrN, TiN) interfaces using the density functional theory. Liu et al. [8] used the density functional theory to study Al/TiN interfaces by calculating electronic distributions and showed that the Al 3sp – N 2s bonds were polar covalent. Lin et al. [9] performed the first principles calculations of the interfacial atomic structure and electronic distribution for aluminum and four kinds of ceramics, TiC, TiN, VC and VN, and found that the bond between an Al and C (or N) atoms stabilize interfaces. Tao et al. [10] selected four metals (Al, Cu, Ti, and Zr) to calculate the adhesion energy of the AlN/metal (Al, Cu, Ti, and Zr) interfaces and showed that the adhesion energy is mainly affected by lattice mismatch and does not have a linear relationship with either formation enthalpy or the surface energy.

Although metal-nitride interfaces have been recently studied, there is less research regarding interfacial structure at the atomic level and the nature of AlN/Ti interface bonding. The effects of microstructure and charge distribution on the interfacial properties of AlN/Ti interfaces need to be further studied.

In this paper, the AlN(0 0 0 1) and Ti(0 0 0 1) surfaces, which are the most close-packed planes in AlN and α-Ti, both with hexagonal structure, were studied. Subsequently, the microstructure, the work of separation and electronic structure of the AlN(0 0 0 1)/Ti(0 0 0 1) interface were studied by the first principles calculations. Furthermore, we systematically investigated the atomic configuration of stable interfaces and the main factors affecting the interfacial mechanical properties.

2. Methodology and calculation details

Total energy and electronic structure calculations as well as the Cambridge serial total energy package (CASTEP), based on the DFT, were used to calculate system energy and electronic structure [11,12]. The self-consistent field procedure was used to solve the Kohn-Sham equation to perform electronic minimization and reach the ground state [13]. Additionally, for atomic structure minimization, the Broyden-Fletcher-Goldfarb-Shanno algorithm (BFGS) was utilized for geometry optimization [14]. The convergence criteria for the maximum energy, force and stress were set as 5×10^{-6} $\frac{eV}{atom}$, 0.01 $\frac{eV}{Å}$, and 0.02 GPa, respectively. For the reaction of different atoms, the selection of valence electrons is significant, which is considered in pseudopotentials for Al: $3s^2$ $3p^1$, N: $2s^2$ $2p^3$ and Ti: $3s^2$ $3p^6$ $3d^2$ $4s^2$. The generalized gradient approximation (GGA) in the Perdew, Burke and Ernzefhof (PBE) method described electron exchange and correlation energy [15]. The convergence tests of plane-wave cutoff energy and the Monkhorst–Pack k-point grid were calculated by evaluating the dependence of system energy on both parameters [16]. Consequently, the plane-wave cutoff energy of 400 eV, the k-point mesh of 9 × 9 × 4 for bulk and 9 × 9 × 1 for surface and interface were utilized in this work.

In order to evaluate the accuracy of the adopted parameters, certain calculations of the bulk properties were first performed. The calculated lattice constants are: a = b = 2.941 Å, c = 4.663 Å for α-Ti bulk, which is similar to the calculated values (a = b = 2.864 Å, c = 4.536 Å [17]) and its experimental values (a = b = 2.951 Å, c = 4.679 Å [18]). For AlN bulk, the values of calculated lattice constants (a = b = 3.126 Å, c = 5.008 Å) are generally consistent with the values of the previous report (a = b = 3.1165 Å, c = 4.9956 Å [19]) and the experimental values (a = b = 3.110 Å, c = 4.980 Å [20]). These results demonstrate that the adopted parameters in this work can ensure sufficient accuracy.

3. Results and discussion

3.1. Surface properties

In thermodynamics, the surface energy (γ_s) is commonly used to define the energy per unit area required to form a new surface and describe the surface stability [21,22]. It is usually obtained according to the following formula [23,24]:

$$\gamma_s = [E_{slab}(N) - NE_{bulk}]/2A_s \quad (1)$$

Here, $E_{slab}(N)$ is the total energy per surface structure, N is the number of atoms in the slab, E_{bulk} is the bulk energy per atom, A_s is the area of corresponding slab surface, and the factor 2 indicates the presence of two identical surfaces of the slab.

The surface is modeled by a slab, which has a certain surface area and a thickness that is thick enough to exhibit bulk-like behavior. To evaluate an applicable thickness for modeling a bulk-like Ti(0 0 0 1) slab and AlN(0 0 0 1) slab, convergence tests are performed in preparation for the following calculations. Due to surface structure, a greater thickness and a larger number of atoms will have more accurate calculation results, however, the calculation process will require more time, memory and hardware resources. Therefore, a reasonable scheme has been executed for convergence tests to choose atom layers by calculating clean surface energy with respect to increasing atom layer thickness. In the slab supercell, two surfaces of the slab with periodic cell structure were separated with a 15 Å vacuum layer to avoid the superfluous influence along the surface and the interface. During this work, the surface energy (γ_s) of AlN(0 0 0 1) and Ti(0 0 0 1) with different thickness slabs was calculated, respectively. Upon attaining a critical thickness, the surface energy will approach a constant value. As shown in Table 1, AlN(0 0 0 1) slab with more than twelve atomic layers almost converges to a constant value of 7.86 J/m^2 and the Ti(0 0 0 1) slab with more than ten atom layers converges to a constant value of 1.94 J/m^2. Therefore, the AlN(0 0 0 1) slab with twelve layers and Ti (0 0 0 1) slab with ten layers are utilized in the following surface and interface calculations to ensure the bulk-like behavior.

It is worth noting that previous AlN(0 0 0 1), which is a stoichiometric slab, has Al- and N-terminated atoms at the top and the bottom, respectively. If the surface layer number is even, the surface energy (γ_s) is exactly the average value of the simultaneously present two terminations and can be quickly calculated from Eq. (1), i.e. $\gamma_{s,AlN(0001)} = (\gamma_{s,AlN(0001)-Al} + \gamma_{s,AlN(0001)-N})/2$. If both sides of the surface are formed by the same single element, Eq. (1) represents the chemical potential of the element. Thus, the surface energy of AlN(0 0 0 1) with non-stoichiometric feature can be given by [25]:

$$\gamma_{AlN} = [E_{slab} - N_{Al}\mu_{AlN}^{bulk} - (N_{Al} - N_N)\mu_N]/A \quad (2)$$

Here, A is the surface area of AlN(0 0 0 1), E_{slab} is the total energy of surface slab, N_{Al} and N_N are the number of Al and N atoms in the surface slab, respectively. μ_{AlN}^{bulk} stands for the chemical potential of AlN bulk and μ_N represents the chemical potential of N element in the surface

Table 1
Convergence of the AlN(0 0 0 1) and Ti(0 0 0 1) surface energy with respect to slab thickness.

Number of layers, n	Surface energy, J/m^2	
	AlN(0 0 0 1)	Ti(0 0 0 1)
4	7.61	1.94
6	7.76	1.96
8	7.73	1.96
10	7.79	1.94
12	7.83	1.94
14	7.83	1.94
16	7.83	1.94

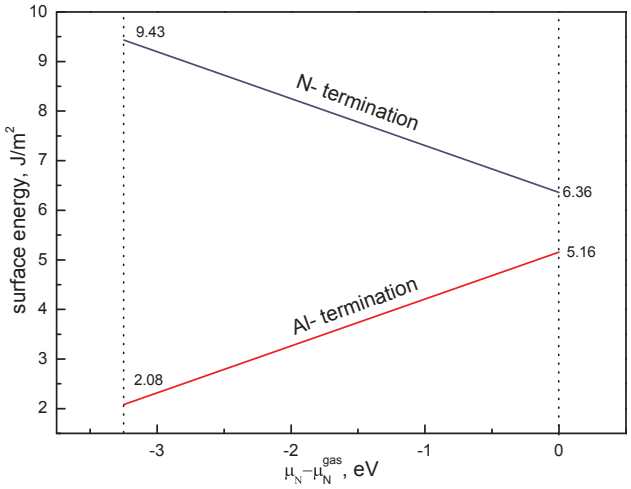

Fig. 1. The relation between surface energies of the N-terminated and Al-terminated AlN(0 0 0 1) and $\mu_N-\mu_N^{gas}$.

slab.

The details of the study method were presented in reports [26–28]. The surface energy for Al- and N-terminated AlN(0 0 0 1) surfaces are a function of nitrogen chemical potential according to Eq. (2). The range of the N chemical potential is [26–28]

$$\Delta H_f^o \le \mu_N-\mu_N^{gas} \le 0 \quad (3)$$

Here, the value of ΔH_f^o is the formation enthalpy of bulk AlN, which is calculated to be 3.248 eV, compared to the Material Project database value of 3.19 eV [29]. The calculation $\mu_N-\mu_N^{gas}$ is the difference of N chemical potential in AlN(0 0 0 1) surface slab and in pure N_2 bulk. The results of surface energy with non-stoichiometric features as a function of nitrogen chemical potential according to Eq. (2) are shown in Fig. 1. If both sides of the surface are the same single element, for the N- and Al-terminated AlN(0 0 0 1), γ_s is in the 6.38–9.43 J/m^2 and 2.08–5.18 J/m^2 ranges, respectively. Furthermore, the surface energy of the both N-terminated AlN(0 0 0 1) is larger than the Al-terminated AlN(0 0 0 1) over the whole range. Additionally, it is common for a surface with a larger surface energy to appear more reactive [30]. Surfaces with higher surface energy create stronger interfacial adhesive properties.

3.2. Interface

Based on the convergence tests of the surface, the 12-layer AlN (0 0 0 1) slab and 10-layer Ti(0 0 0 1) slab are used to build the AlN (0 0 0 1)/Ti(0 0 0 1) interface with 15 Å vacuum layers, in which the two close-packed planes are matched to form the interface. According to this lattice orientation, the mismatch between AlN is about 3.15%, which has a small effect on the calculation of the AlN /Ti interface properties. Separation distance d_0 greatly affects W_{sep} and interfacial atomic bonding. Therefore, a value of 1.5–2 Å was selected for d_0 in accordance with previous reports [10,31,32].

The AlN(0 0 0 1) slabs with Al- and N-terminations are studied with fully relaxed in all directions in the interface. Meanwhile, the different interfacial stacking sequences have been considered, which different in the position of interfacial Ti atoms with respect to the AlN(0 0 0 1) slab lattice structure shown in Fig. 2, where there are three different staking sequences. The OT sequence describes the interfacial Ti atoms of the Ti (0 0 0 1) slab, directly located at the top of N or Al atom of the AlN slab. The SL sequence describes the interfacial Ti atoms located at the top of N or Al atoms of the second layer of the AlN(0 0 0 1) slab. The TL sequence describes the interfacial Ti atoms located at the top of N or Al atoms of the third layer of the AlN(0 0 0 1) slab. Consequently, a total of six different interfacial configurations were considered.

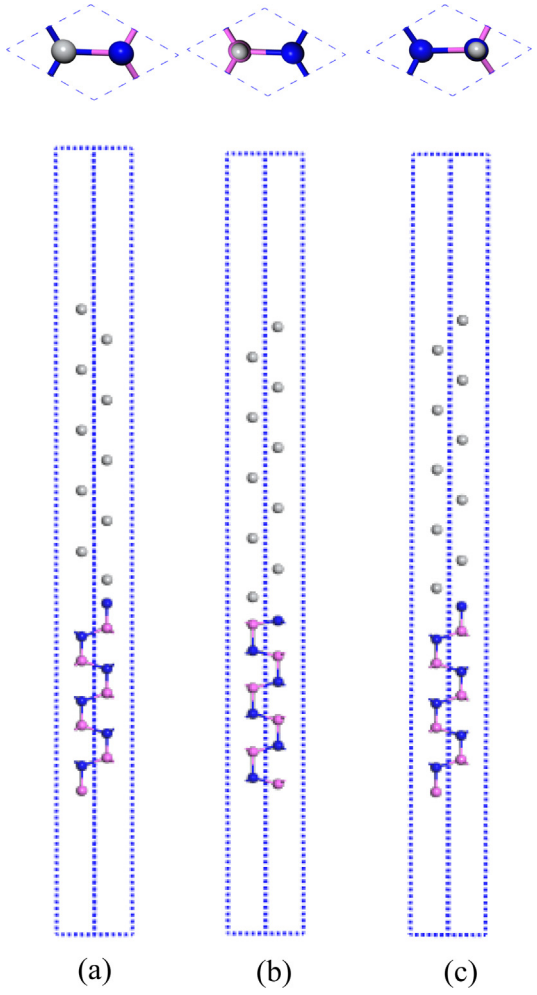

Fig. 2. Top views and side views of three stacking sequences for N-terminated AlN(0 0 0 1)/Ti(0 0 0 1) interface: (a) OT, (b) SL, and (c) TL stacking sequences. Three atoms layers are shown, in which the pink spheres are interfacial Al atom, the blue spheres are N atom and the grey spheres are Ti atom.

3.3. Interface structure and work of separation

The work of separation W_{sep} has been calculated. It is an important fundamental value to represent the adhesive properties and is defined as the reversible work required to cleave an interface into two free surfaces. It can be estimated using the total energy difference between the interface and its isolated surface slabs [33]:

$$W_{sep} = \frac{E_{slab,\alpha} + E_{slab,\beta} - E_{int}}{A} \quad (4)$$

Here, $E_{slab,\alpha}$ and $E_{slab,\beta}$ are the total energy of relaxed surface slabs and the subscripts α and β are materials α and β. E_{int} is the total energy of the interface system and A is the interface area of the unit cell.

As seen from Table 2, the W_{sep} values for six interface configurations of the two terminations have been listed with corresponding interface distance d_0. The N-terminated interfaces present larger W_{sep} and smaller interfacial distance d_0 than Al-terminated interfaces. This phenomenon may be explained by the higher surface energy of N-terminated interfaces, which is greater than Al-terminated surfaces. This results in more activity, more reactions and easier bond formation. On the other hand, the stacking sequence is an influencing factor affecting W_{sep}. Of all the equilibrium stable interface geometries, the highest W_{sep} values of 13.19 J/m^2 and 13.34 J/m^2 were calculated for the OT and TL stacking of the N-terminated interface. As expected, the TL stacking geometry for the N-terminated interface is preferred, as it

Table 2
Work of separation (W_{sep}) and interfacial distance (d_0) for the relaxed AlN (0 0 0 1)/Ti(0 0 0 1) interfaces.

Termination	Stacking	d_o, Å	W_{ad}, J/m^2
N	OT	0.83	13.19
	SL	1.92	1.72
	TL	0.81	13.34
Al	OT	2.15	1.04
	SL	2.37	4.44
	TL	2.16	1.31

almost extends the bulk AlN stacking sequence across the interface into the metal [7]. Comparing the TL stacking of N-terminated interface, the initial OT stacking sequence for N-terminated interface is quite different with bulk AlN sequence. After full relaxation, this interface configuration is reconstructed closer to the TL stacking sequence for the N-terminated interface with shorter interface distance (d = 0.81 Å). Therefore, OT stacking sequence of the N-terminated interface has a value of W_{sep}, which is the same as the TL stacking value. For the interface with N-termination, the TL is the most favorable structure. For the interface with Al-termination, the SL model (W_{sep} = 4.44 J/m^2) indicates the most favorable structure. Therefore, for study the local interface structure and interface bonding, the following section of the paper will mainly discuss the N-terminated interfaces with the TL structure and Al-terminated with SL.

3.4. Electronic structure and bonding

The adhesion strength of the metal/ceramic interface is most determined by the bond strength. So study the bonding nature is necessary in the interface using electronic structures. Furthermore, the most stable interfaces for the TL stacking sequence of N-terminated and SL stacking sequence of Ti-terminated interfaces were investigated by difference charge densities, i.e. the density of states (DOS).

The difference charge density $\Delta\rho$ is presented:

$$\Delta\rho = \rho_{AlN/Ti} - \rho_{AlN} - \rho_{Ti} \quad (5)$$

Here, $\rho_{AlN/Ti}$ is the charge density of the AlN/Ti interface, ρ_{AlN} and ρ_{Ti} are the total charge density of the AlN and Ti slabs with the same unit cell, respectively.

Fig. 3 shows the charge density and the difference in charge density for the TL staking of N-terminated interface and for the SL staking of Al-terminated interface. There are some obvious differences in the interfacial electronic structure of the two interfaces, which illustrate significant interfacial bonding characters. First, the charge transfers at the TL staking of N-terminated interface can see in Fig. 3(a), where the charge transfers come mainly from interfacial Ti to N atoms with more strength than the charge transfer comes from the Al-terminated interface with SL stacking between Al and Ti atoms. Therefore, the N and Ti atoms have formed stronger chemical bonds in accordance with the W_{sep} value in Table 2. Second, from Fig. 3(b) and (d), the charge distributions for N and Ti atoms are very similar. While both show high charge accumulation and spherical symmetry characteristics, there is obvious charge depletion in the Al atom. For the Al-terminated interface with SL stacking, a few charge accumulation is between the interfacial Al and Ti atoms. On the side, a large amount of charge accumulation between interfacial N and Ti atoms occurred in the N-terminated interface with TL stacking. As a result, a covalent bond can be found between the neighboring N atom and Ti atom forming the N—Ti bond, and the neighboring Al and Ti atom forming the Al—Ti bond. Evidently, the covalent interaction for the N—Ti bond is stronger than the Al—Ti bond. Both the TL staking of N-terminated and SL staking of Al-terminated interfaces show a mix of covalent and ionic bonding.

For a deeper insight into electronic structure and the nature of bonding for the N-terminated interface with TL sequence and Al-terminated interface with SL sequence, the partial densities of states plots are presented in Figs. 4 and 5, respectively. The left chart presents the PDOS of the AlN layer and the right chart presents those of the Ti layer, where the 1st layer is located in the interface area.

For the N-terminated interface with TL sequence, there are some interesting features in Fig. 4. The PDOS of the 1st Ti layer of the Ti slab shows that the electronic occupied states move to lower energy, causing the peak position of Ti-d orbital to decrease by 2 eV compared with the inner Ti. Simultaneously, the occupied states of interfacial N atom (1st N layer) move to high energy, causing its N-p peak position to increase by 2 eV compared with the same atoms in the inner layer. This effect is more localized at the exterior layer than for the interior layer for the same atoms shown in Fig. 4. Furthermore, the PDOS of interfacial Ti atoms in the Ti(0 0 0 1) slab, especially for the Ti-d orbital, appear to peak at around −4 eV, and this peak is overlapped with the peak of interfacial N atoms in the AlN(0 0 0 1) slab, especially with N-p orbitals. These overlapping states indicate that the hybridization of the Ti and N orbitals, especially Ti-d and N-p, formed a strong covalent interaction.

Fig. 5 shows the partial density of states for the Al-terminated interface with the SL sequence, where the curves of the 1st Al layer are quite flat and non-localized, and occur in the wide energy range. This shows more metallic features than the inner Al layer, which suggests that the metallic bond has formed between Ti and Al at the interface area. Moreover, the PDOS of Ti atoms in the first Ti(0 0 0 1) layer show a peak around −1 eV, and this peak is overlapped with one of the first Al layer of AlN(0 0 0 1), but the overlap between them is relatively small. As a result, for the Al-terminated interface with the SL sequence, the interfacial bonds suggest less covalent features compared the N-interface with the TL sequence. All charge changes mainly occur in the first two layers, while the state of the other layers remains unchanged, consistent with the central layer, therefore, this evidence indicates that the first two layers of atoms play an incomparable role in the interface properties, and the type and arrangement of interface atoms greatly influence adhesion of the interface.

In summary, for the N-terminated interface with TL sequence, the main interfacial bonding interaction is the strong covalent bond, produced mainly by the orbital hybridization of N-p and Ti-d. For the Al-terminated interface with the SL sequence, the interfacial interaction is mainly the metallic bond and partial weak covalent bond. This is very similar to the result of charge density and difference charge density.

4. Conclusions

The first principles calculations based on density functional theory were calculated to obtain the work of separation, stable interface structure and the interfacial bonds for the AlN(0 0 0 1)/Ti(0 0 0 1) interfaces. Considering the two terminations of AlN(0 0 0 1) (Al-terminated and N-terminated) and different stacking sequences (OT-, SL- and TL-sequence), six constructed interface models were investigated. The following conclusions can be drawn.

(1) Surface convergence tests show that the AlN(0 0 0 1) slab contains more than twelve atomic layers, and the Ti(0 0 0 1) slab contains more than ten atomic layers. The corresponding surface energy γ_s converges to 7.86 J/m^2 and 1.94 J/m^2, respectively.
(2) The N-terminated interfaces present bigger W_{sep} and shorter interfacial distance d_0 than the Al-terminated interface. Of all the equilibrium interface geometries, the largest W_{sep} values of 13.19 J/m^2 and 13.34 J/m^2 were calculated for the OT and TL stacking of the N-terminated interface, respectively.
(3) The stacking sequence strongly affects W_{sep}, in which the TL stacking sequence for the N-terminated interface shows the highest stability. For the Al-terminated interface, the SL stacking sequence exhibit s most stable.
(4) The TL stacking geometry for the N-terminated interface is

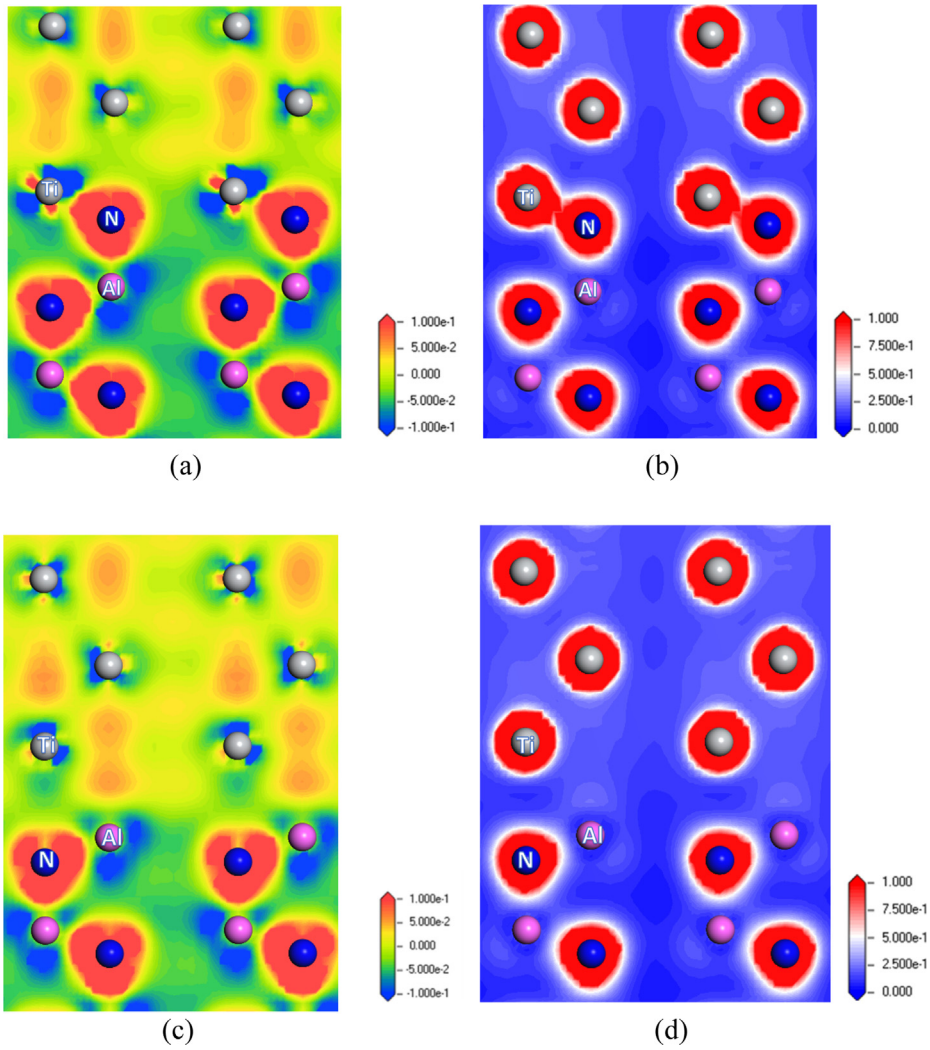

Fig. 3. Difference charge density (a) and charge density (b) for the TL staking of N-terminated interface, difference charge density (c) and charge density (d) for the SL staking of Al-terminated interface, red and blue areas represent charge increase and decrease respectively. Dotted line indicates the interface location.

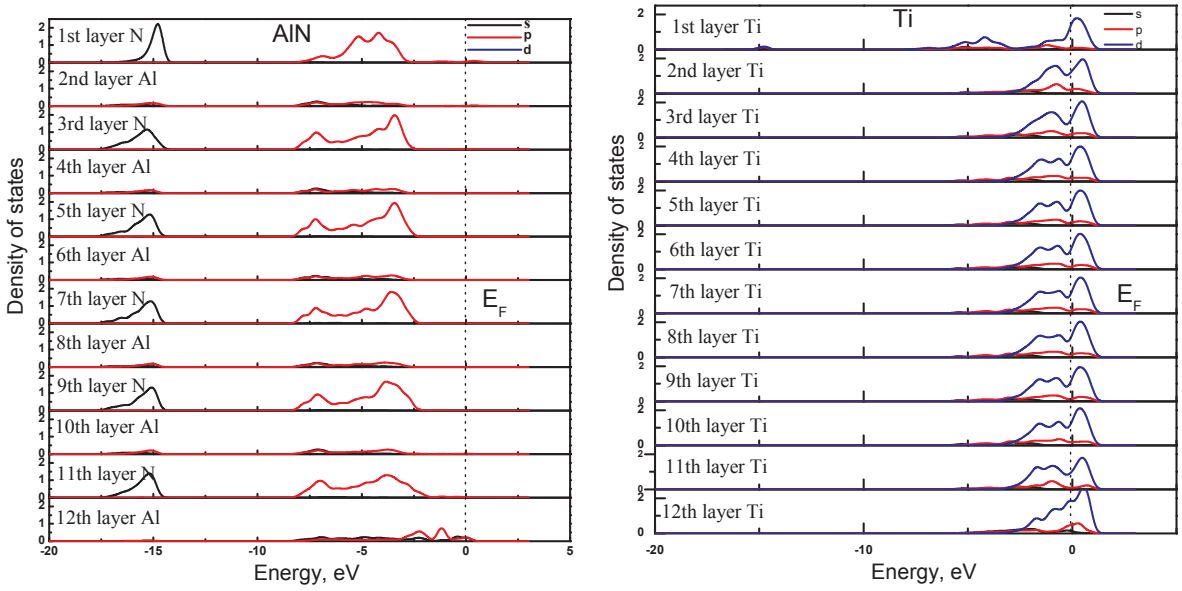

Fig. 4. Partial density of states (PDOS) for the N-interface with TL sequence.

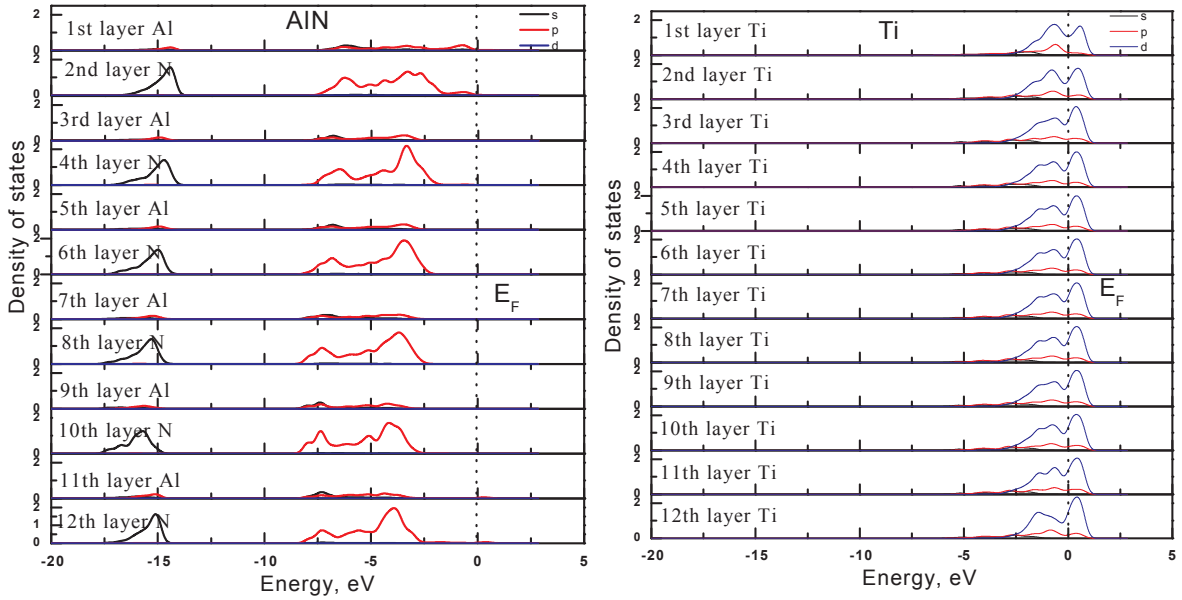

Fig. 5. Partial density of states (PDOS) for the Al-terminated interface with SL sequence.

preferred, as it almost extends the bulk AlN stacking sequence across the interface and into the metal.

(5) The results of charge density and charge density difference show that the covalent bond can be formed at the N—Ti and Al—Ti interfaces. Evidently, the covalent interaction for the N—Ti bond is stronger than the Al—Ti bond. Both TL staking of the N-terminated and the SL staking of the Al-terminated interfaces show a mix of covalent and ionic bonding.

(6) The partial density of states (PDOS) indicate that for the N-terminated interface with the TL sequence, the interfacial bond is the strong covalent bond contributed mainly by the orbital hybridization of N-p and Ti-d. For the Al-terminated interface with the SL sequence, the interfacial interaction is mainly the metallic bond and partial weak covalent bond. This may be the reason that the N-terminated interface with the TL sequence revealed higher interfacial stability than the Al-terminated interface with the SL sequence.

Acknowledgements

This work was supported by the Beijing Nova Program (Z171100001117075), the National Natural Science Foundation of China (51771025), and the Fundamental Research Funds for the Central Universities (FRF-TP-17-002C1).

Appendix A. Supplementary material

Supplementary data to this article can be found online at https://doi.org/10.1016/j.cplett.2018.10.034.

References

[1] J. Schulz-Harder, Advantages and new development of direct bonded copper substrates ☆, Microelectron. Reliab. 43 (3) (2003) 359–365.
[2] H. Ru, V. Wei, T. Jiang, M. Chiu, Direct plated copper technology for high brightness LED packaging, Microsystems, Packaging, Assembly and Circuits Technology Conference, 2011, pp. 311–314.
[3] L. Dupont, Z. Khatir, S. Lefebvre, S. Bontemps, Effects of metallization thickness of ceramic substrates on the reliability of power assemblies under high temperature cycling, Microelectron. Reliab. 46 (9–11) (2006) 1766–1771.
[4] C.H. Lin, P.S. Huang, M.Y. Tsai, C.T. Wu, Mechanical design and analysis of direct plated copper film on AlN substrates for thermal reliability in high power module applications, International Conference on Electronic Packaging and Imaps All Asia Conference, 2015, pp. 185–188.
[5] H.-C. (Jay) Yu, J. Huang, Investigation of the direct plating copper (DPC) on Al_2O_3, BeO or AlN ceramic substrates for high power density applications, Int. Symp. Microelectron. 2016 (1) (2016) 000079–000086.
[6] V. Wei, M. Huang, R. Lai, R. Persons, A comparison study for metalized ceramic substrate technologies: For high power module applications, 2014 9th International Microsystems, Packaging, Assembly and Circuits Technology Conference (IMPACT), 2014, pp. 141–145.
[7] D.J. Siegel, L.G. Hector, J.B. Adams, Ab initio study of Al-ceramic interfacial adhesion, Phys. Rev. B 67 (9) (2003) 092105.
[8] L.M. Liu, S.Q. Wang, H.Q. Ye, Adhesion of metal–carbide/nitride interfaces: Al/TiC and Al/TiN, J. Phys. Condens. Matter 15 (47) (2003) 8103.
[9] Z. Lin, X. Peng, T. Fu, Y. Zhao, C. Feng, C. Huang, Z. Wang, Atomic structures and electronic properties of interfaces between aluminum and carbides/nitrides: a first-principles study, Phys. E Low-Dimens. Syst. Nanostructures 89 (2017) 15–20.
[10] Y. Tao, G. Ke, Y. Xie, Y. Chen, S. Shi, H. Guo, Adhesion strength and nucleation thermodynamics of four metals (Al, Cu, Ti, Zr) on AlN substrates, Appl. Surf. Sci. 357 (Dec. 2015) 8–13.
[11] M.D. Segall, P.J.D. Lindan, M.J. Probert, C.J. Pickard, P.J. Hasnip, S.J. Clark, M.C. Panyne, First-principles simulation: ideas, illustrations and the CASTEP code, J. Phys. Condens. Matter 14 (11) (2002) 2717.
[12] D. Vanderbilt, Soft self-consistent pseudopotentials in a generalized eigenvalue formalism, Phys. Rev. B 41 (11) (Apr. 1990) 7892–7895.
[13] W. Kohn, Density functional and density matrix method scaling linearly with the number of atoms, Phys. Rev. Lett. 76 (17) (Apr. 1996) 3168–3171.
[14] T.H. Fischer, J. Almlof, General methods for geometry and wave function optimization, J. Phys. Chem. 96 (24) (Nov. 1992) 9768–9774.
[15] J.P. Perdew, K. Burke, M. Ernzerhof, Generalized gradient approximation made simple, Phys. Rev. Lett. 77 (18) (Oct. 1996) 3865–3868.
[16] H.J. Monkhorst, J.D. Pack, Special points for Brillouin-zone integrations, Phys. Rev. B 13 (12) (1976) 5188–5192.
[17] M. Jafari, N. Zarifi, M. Nobakhti, A. Jahandoost, M. Lame, Pseudopotential calculation of the bulk modulus and phonon dispersion of the bcc and hcp structures of titanium, Phys. Scr. 83 (6) (2011) 065603.
[18] A.Y. Kuksin, A.S. Rokhmanenkov, V.V. Stegailov, Atomic positions and diffusion paths of h and he in the α-Ti lattice, Phys. Solid State 55 (2) (Feb. 2013) 367–372.
[19] Z.Q. Liu, J. Ni, The electronic properties of SiCAlN quaternary compounds, Eur. Phys. J. B 59 (1) (2007) 29–34.
[20] H. Schulz, K.H. Thiemann, Crystal structure refinement of AlN and GaN, Solid State Commun. 23 (11) (Sep. 1977) 815–819.
[21] Q. Jiang, D.S. Zhao, M. Zhao, Size-dependent interface energy and related interface stress, Acta Mater. 49 (16) (2001) 3143–3147.
[22] E. Artacho, J. Zegenhagen, Surface energy and stability of stress-driven discommensurate surface structures, Phys. Rev. B 52 (23) (1995) 16373.
[23] D.P. Sigumonrong, D. Music, J.M. Schneider, Efficient supercell design for surface and interface calculations of hexagonal phases: α-AlO case study, Comput. Mater. Sci. 50 (3) (2011) 1197–1201.
[24] H.S. Abdelkader, H.I. Faraoun, Ab initio investigation of Al/MoB interfacial adhesion, Comput. Mater. Sci. 50 (3) (2011) 880–885.
[25] J. Yang, X. Hou, P. Zhang, Y. Zhou, X. Xing, X. Ren, Q. Yang, First-principles calculations on $LaAlO_3$ as the heterogeneous nucleus of austenite, Comput. Theor. Chem. 1029 (2014) 48–56.
[26] D.J. Siegel, L.G.H. Jr, J.B. Adams, Adhesion, stability, and bonding at metal/metal-carbide interfaces: Al/WC, Surf. Sci. 498 (3) (2002) 321–336.
[27] L.M. Liu, S.Q. Wang, H.Q. Ye, First-principles study of polar Al/TiN(1 1 1)

interfaces, Acta Mater. 52 (12) (2004) 3681–3688.
[28] K. Li, Z.G. Sun, F. Wang, N.G. Zhou, X.W. Hu, First-principles calculations on Mg/Al_4C_3 interfaces, Appl. Surf. Sci. 270 (Apr. 2013) 584–589.
[29] A. Jain, S.P. Hautier, W. Chen, W.D. Richards, S. Cholia, D. Gunter, D. Skinner, G. Ceder, K.A. Persson, Commentary: the materials project: a materials genome approach to accelerating materials innovation, APL Mater. 1 (1) (2013) 011002.
[30] S.V. Dudiy, J. Hartford, B.I. Lundqvist, Nature of metal-ceramic adhesion: computational experiments with Co on TiC, Phys. Rev. Lett. 85 (9) (Aug. 2000) 1898–1901.
[31] C. Liu, N. Jin, Z. Li, X. Liu, First-principles calculations on the electronic structure and bonding nature of TaN(111)/TiN(111) interface, J. Alloys Compd. 717 (Sep. 2017) 326–332.
[32] X.-Y. Xu, H.-Y. Wang, M. Zha, C. Wang, Z.-Z. Yang, Q.-C. Jiang, Effects of Ti, Si, Mg and Cu additions on interfacial properties and electronic structure of Al(111)/4H-SiC(0001) interface: a first-principles study, Appl. Surf. Sci. 437 (Apr. 2018) 103–109.
[33] M.W. Finnis, The theory of metal – ceramic interfaces, J. Phys. Condens. Matter 8 (8) (1996) 5811.